

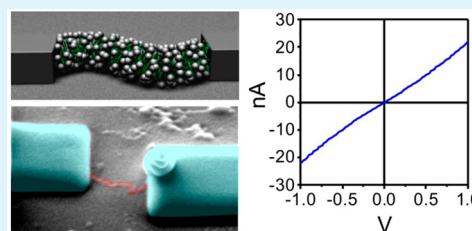
Conductive Nanowires Templated by Molecular Brushes

Ivan Raguzin,^{†,‡} Manfred Stamm,^{†,‡} and Leonid Ionov^{*,†,§}[†]Leibniz Institute of Polymer Research e.V. Dresden, Hohe Str. 6, D-01069 Dresden, Germany[‡]Technische Universität Dresden, Fakultät Mathematik und Naturwissenschaften, 01062 Dresden, Germany[§]University of Georgia, Athens, Georgia 30602, United States

Supporting Information

ABSTRACT: In this paper, we report the fabrication of conductive nanowires using polymer bottle brushes as templates. In our approach, we synthesized poly(2-dimethylamino)ethyl methacrylate methyl iodide quaternary salt brushes by two-step atom transfer radical polymerization, loaded them with palladium salt, and reduced them in order to form metallic nanowires with average lengths and widths of 300 and 20 nm, respectively. The obtained nanowires were deposited between conductive gold pads and were connected to them by sputtering of additional pads to form an electric circuit. We connected the nanowires in an electric circuit and demonstrated that the conductivity of these nanowires is around $100 \text{ S}\cdot\text{m}^{-1}$.

KEYWORDS: bottle brushes, template, nanowire, conductive, ATRP



INTRODUCTION

Conductive nanowires are highly interesting objects with great importance for nanotechnology because they allow substantial miniaturization of electric circuits,^{1,2} which can be applied for the design of sensors,³ as well as in optoelectronics⁴ and photonics.⁵ Moreover, conductive nanowires are interesting due to their unique optical,⁶ magnetic,⁷ and catalytic⁸ properties. One approach for the fabrication of nanowires is the use of intrinsically nonconductive structures as templates and subsequently covering them with conductive materials or converting them into one by metallization or carbonization. For example, several approaches have been developed to synthesize metallic nanowires such as template synthesis,^{9–11} step-edge decoration,¹² and vapor–liquid–solid condensation,¹³ as well as several other wet chemical techniques based on the reduction of metal ions in the presence of protecting polymers or surfactants.⁹ Template-based methods involve deposition of metals into cylindrical pores of a host material, so-called 1D nanotemplates, e.g., carbon nanotubes,¹⁴ rod-like micelles,¹⁵ etc.

Molecular bottle brushes, polymer molecules with multiple poly or oligomer chain side groups, are a brilliant example of such structures that can be used as templates.^{16,17} In fact, they can be synthesized in a variety of topologies such as bi- or multiblock, stars, etc. that allows design of nanostructures with different topology. Moreover, in contrast to linear polymer molecules, which are typically coiled and adopt extended conformation only when the molecules are strongly charged,^{18–20} bottle brushes are often stretched due to strong steric repulsion between the massive side groups. Additionally, polymer side chains could be designed in a way that they form complexes with metal ions, a property that can be used for loading of a considerable amount of conductive species on

them. Despite several reports on the use of bottle brushes for templating of semiconducting materials,^{21,22} metal clusters, and nanowires,^{23–25} to our best knowledge, there are no reports on the conductive properties of nanostructures based on bottle brushes. Here, for the first time, the design of metallic nanowires by using polymer bottle brushes as templates and the investigation of their conductive properties is reported.

EXPERIMENTAL SECTION

Materials. α -Bromoisobutryl bromide (Aldrich, 98%), ethylene bis(2-bromoisobutyrate) (Aldrich, 97%), 4,4'-dinonyl-2,2'-dipyridyl (dN bpy, Aldrich, 97%), copper(I) bromide (CuBr, Aldrich, 99.999%), copper(II) bromide (CuBr₂, Aldrich, 99.999%), potassium fluoride (Sigma-Aldrich, $\geq 99.0\%$), L-ascorbic acid (Aldrich, 99+%), *N,N,N',N',N'*-pentamethyldiethylenetriamine (PMDTA, Aldrich, 99%), tetrabutylammonium fluoride solution (Aldrich, 1.0 M in THF), iodomethane (Aldrich, 99.5%), ethanol abs. (EtOH, VWR, 99.9%), tetrahydrofuran (Acros, 99.99%), hexane (Aldrich, 95%), and *N,N*-dimethylformamide (DMF, Aldrich, anhydrous, 99.8%) were used as received. 2-(Trimethylsilyloxy)ethyl methacrylate (HEMA-TMS, Aldrich) and 2-(dimethylamino)ethyl methacrylate (DMAEMA, Aldrich) were passed through basic and neutral aluminum oxides prior to polymerization.

Scanning Electron Microscopy (SEM). All scanning electron microscopy (SEM) images were acquired on a NEON 40 EsB CrossBeam scanning electron microscope from Carl Zeiss NTS GmbH, operating at 3 keV in the secondary electron (SE) mode.

PeakForce TUNA. AFM images were taken with a Bruker Dimension Icon AFM (Bruker, USA). Cantilevers with conductive coating of 5 nm chromium and 25 nm of platinum with force constant of 3 N/m were used (ElectriMulti75-G).

Received: August 21, 2015

Accepted: September 25, 2015

Published: September 29, 2015

Cryogenic Transmission Electron Microscopy (Cryo-TEM).

Cryogenic TEM images were acquired on a Libra 120 cryo-TEM from Carl Zeiss NTS GmbH equipped with a LaB₆ source. The acceleration voltage was 120 kV, and the energy filter with an energy window of 15 eV was used.

P(HEMA-TMS), Poly(2-(trimethylsilyloxy)ethyl Methacrylate). Ethylene bis(2-bromoisobutyrate) (4.9 mg, 0.0136 mmol) and dNbpv (25.3 mg, 0.062 mmol) were mixed in a Schlenk flask. The mixture was purged with argon three times, and deoxygenated HEMA-TMS (5 g, 24.71 mmol) and DMF (1.5 mL) were transferred into the flask using a cannula. The resulting solution was degassed by three freeze–pump–thaw cycles. The mixture was stirred for 30 min at room temperature, and after that, CuBr (4.5 mg, 0.031 mmol) was added. The flask was placed in a thermostated oil bath at 70 °C. After 15 h, the polymerization was stopped by cooling the mixture to room temperature and opening the flask. The mixture was diluted with THF and passed through basic Al₂O₃. The solvent and the rest of the monomer were removed using a rotary evaporator, and the resultant polymer was dried in an oven at 40 °C under vacuum (yield 82%).

¹H NMR (δ, ppm, CDCl₃): 0.14 s (9H, Si–CH₃); 0.90–1.05 overlapped (3H, CH₃); 1.81–1.90 overlapped (2H, CH₂); 3.75 br. s (2H, CH₂); 4.00 br. s (2H, CH₂).

PBiBEMA, Poly(bromo-isobutyrylethyl Methacrylate). Tetrabutylammonium fluoride (0.013 g, 0.05 mmol) was added dropwise to a mixture of pHEMA-TMS (1 g, 4.95 mmol) and KF (0.287 g, 4.95 mmol) in anhydrous THF (50 mL), followed by a slow addition of 2-bromoisobutyryl bromide (1.6 g, 7.43 mmol) over a course of 30 min. The reaction mixture was stirred overnight at room temperature and precipitated in methanol–ice (80/20 v/v%). The obtained precipitate was dissolved in chloroform, passed through basic Al₂O₃, and reprecipitated in hexane. The polymer was dried in a vacuum oven at 30 °C giving 0.84 g of pBiBEMA (60.8%).

¹H NMR (δ, ppm, CDCl₃): 0.90–1.08 overlapped (3H, CH₃); 1.84–1.93 overlapped (2H, CH₂); 1.97 s (6H, CH₃); 4.21 br. s (2H, CH₂); 4.37 br. s (2H, CH₂).

PDMAEMA Brushes. In a 10 mL test tube 2-(dimethylamino)-ethyl methacrylate (DMAEMA) (2 g, 12.74 mmol), ethanol (2 mL), copper(II) bromide (32 μL of a 0.1 M solution in DMF), N,N,N',N'',N''-pentamethyldiethylenetriamine (32 μL of a 0.5 M solution in DMF), pBiBEMA (6 mg, 0.018 mmol), and ascorbic acid (50 μL of a 1 M solution in DMF) were mixed. The test tube was placed in a thermostated oil bath at 70 °C. After 30 min, the reaction was stopped by cooling down to room temperature and opening the test tube. The resultant mixture was diluted with THF, passed through basic Al₂O₃ and precipitated in diethyl ether. The obtained polymer was dried in a vacuum oven at room temperature (0.12 g, yield 6.28%). The contour length of side chains was estimated using eq 1.

$$L = \frac{m_{\text{brush}} - m_{\text{in}}}{M_{\text{side_groups}}} \cdot \frac{M_{\text{initiator}}}{m_{\text{in}}} \cdot 2.5A \quad (1)$$

where m_{brush} is the mass of the obtained bottle brush, m_{in} is the mass of macroinitiator, $M_{\text{side_groups}}$ is molecular mass of monomer units of side polymer chains, and M_{in} is molecular mass of monomer units of macroinitiator.

qPDMAEMA Brushes. PDMAEMA bottle brushes (0.5 g, 3.185 mmol) were dissolved in ethanol (10 mL), followed by an addition of iodomethane (3 mL). The flask was heated up with a heat gun until all of the polymer precipitated. The mixture was filtered, and the obtained polymer was dried in a vacuum oven at 40 °C (0.85 g, yield 89.26%).

RESULTS AND DISCUSSION

The poly(2-dimethylamino)ethyl methacrylate methyl iodide quaternary salt (qPDMAEMA) bottle brushes (Figure 1a) were synthesized by ATRP using macroinitiators (Figure S1) as described earlier.²⁶ Briefly, the macroinitiator was first synthesized by atom transfer radical polymerization (ATRP). Next, side PDMAEMA chains were grown by a second ATRP. Finally, tertiary amino groups were quaternized by reaction

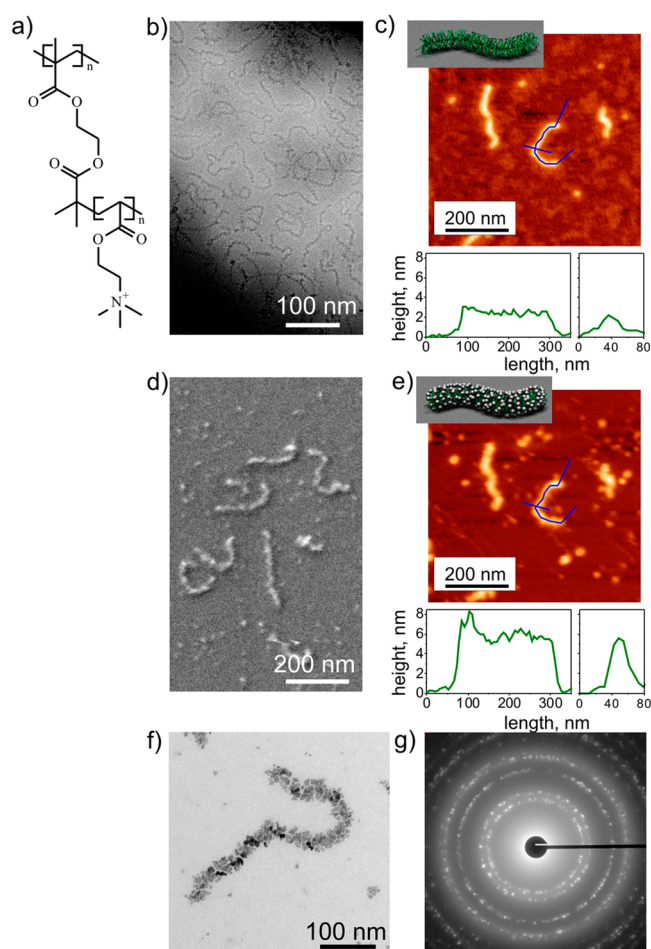


Figure 1. PDMAEMA bottle brushes before and after metallization: (a) structural formula, (b) cryoTEM image, and (c) AFM image of a PDMAEMA brush before metallization; (d) SEM, (e) AFM, and (f) TEM images of metallized bottle brushes; (g) electron scattering pattern on metallized brush from (f).

with CH₃I. As a result, strongly charged qPDMAEMA brushes were obtained.

The qPDMAEMA brushes have stretched conformation in water solutions as it was revealed by CryoTEM (Figure 1b). In CryoTEM images, the chains appear as dark worm-like structures on a gray background, the contrast resulting from the staining effect of heavy I[−] anions associated with positively charged polymer molecules. The qPDMAEMA brushes were spin-coated on freshly cleaved mica sheets from highly diluted aqueous solution (0.02 mg/mL). The adsorbed polymer molecules form stretched worm-like structures due to the electrostatic repulsion of the charged side amino groups (Figure 1c). The average length of the brushes was found to be around 500 ± 100 nm. The contour length of the side groups, estimated by considering the ratio between the amount of obtained polymer and amount of macroinitiator used for polymerization, was found to be 9 nm, that is consistent with results of AFM (Figure 1c). Then, the mica sheets with adsorbed brushes were immersed in a solution of H₂PdCl₄ (0.1 g/L of the Pd(CH₃COO)₂ in HCl, pH 2) for 2 h, to allow the PdCl₄^{2−} ions to penetrate through the dense shell of charged side chains of the bottle brush. After rinsing in water, the palladium chloride ions were reduced to metallic palladium by treatment with a dimethylamine borane solution (1 mg/mL).

We found that the metalization procedure does not change the conformation of the bottle brushes adsorbed on the substrate (Figure 1d,e) but results in an increase in their height from ca. 3 nm (nonmetalized brush) to ca. 6 nm (after metalization, Figure 1e), that indicates the deposition of a new material. We also exposed the sample with metalized brushes to oxygen plasma in order to prove that the increase of height of the brushes is not due to the adsorption of organic molecules but rather because of the formation of metallic clusters. It was found that plasma treatment of metallized brushes led to a very minor decrease in their height (Figure S2), while the nonmetallized brushes completely disappeared (not shown). We performed detailed investigation of the structure of the metalized polymer nanowires using TEM. We found that nanowires consist of multiple nanoparticles with the size ranging between 3 and 10 nm. We also have found by using electron diffraction that the particles have crystalline structure corresponding to metallic Pd.²⁷ The width of metallized nanowire is ca. 35 nm. Thus, treatment with palladium salt solution and their subsequent reduction results in the metalization of bottle brushes and formation of metallized nanowires. It is difficult to say what the distribution of Pd ions in brush is because they penetrate inside or stay on the surface. Moreover, the reduction may change it.

Next, we fabricated an electronic circuit using metalized bottle brushes. For this, we first adsorbed bottle brushes on the surface of a silica wafer between two large gold electrodes (Figure S3) and metalized them (Figure 2a,b). The length of the brush and metallized nanowire based on it was ca. 600 nm, shorter than the gap between the electrodes. Therefore, the nanowire was connected to the electrodes by depositing platinum pads using a focused ion beam (Figure 2c,d). In our

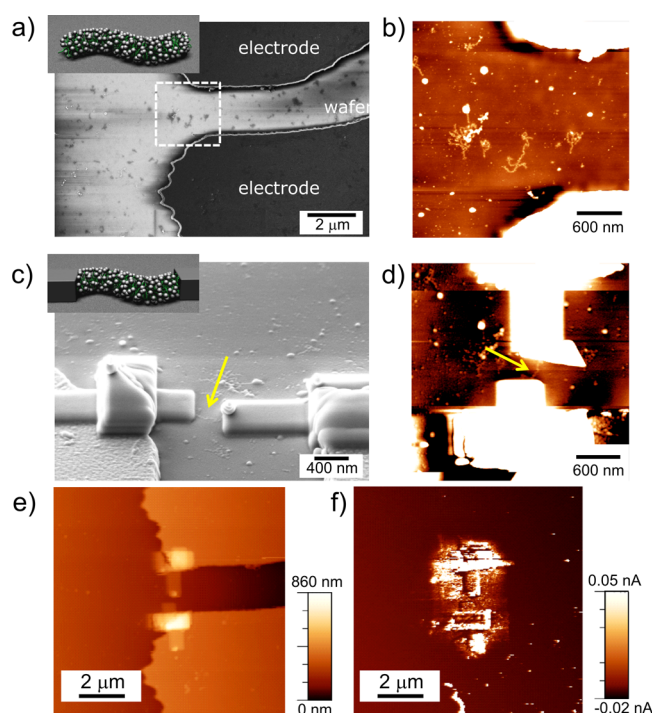


Figure 2. Metallized bottle brush between two electrodes: (a) SEM and (b) AFM images before sputtering of the contacts; (c) SEM and (d) AFM images of the same spot after sputtering of contacts; (e) and (f) topographical (left) and conductivity (right, peak force TUNA) mapping of the area around the sputtered electrodes.

setup, the electrode was sputtered on the end of the brush, and we expect that the resistivity at the point of the contact between the brush and sputtered metal is low. Conductive measurement, performed by using Peak Force TUNA AFM, confirmed this (Figure 2e,f). The surface of nonsputtered gold lines appears to be nonconductive in this experiment. We believe that the reason for this is oxidation of the gold surface by oxygen plasma during the cleaning procedure before the deposition of molecular bottle brushes. However, inside, they remained conductive as it can be seen from the PeakForce. Moreover, golden lines were additionally checked and proved to be conductive. We have also measured conductivity of the sputtered bridge and sputtered gap as references. Electrical characterization of the specimens was performed on a Keithley device. According to the results, all three samples were conductive and showed a linear voltage–current dependency with different inclination, i.e., resistivity (Table 1, Figure 3). The surface for the “gap” measurements was treated with Pd in the same way as the sample in Figure 3c. Moreover, the electrodes were located/formed on the different areas of the same golden chip, which fully exclude different surface preparations. The resistance of the nanowire (48 MΩ) was much lower than that of the gap (606 MΩ) and higher than that of the bridge (0.86 MΩ). We also estimated the conductivity of the obtained nanowire and the bridge. The conductivity of the nanowire was calculated by considering the cross-sectional area of the metal deposited on the brush, which was retrieved from AFM thickness measurements as well as TEM and was around 64 nm². Therefore, considering the length of the brush between the sputtered electrodes (around 300 nm), it was also possible to estimate the conductivity of one single brush, which was $\sim 98 \text{ S}\cdot\text{m}^{-1}$. The conductivity of the bridge was found to be $167 \text{ S}\cdot\text{m}^{-1}$. We performed 3 independent experiments, which showed similar results of conductivity of Pd nanowires. Both values are however considerably lower than the electric conductivity of bulky platinum and solid continuous nanowires, which is $10^7 \text{ S}\cdot\text{m}^{-1}$.²⁸ On the other hand, the conductivity of our Pd nanowires is close to the conductivity of silver nanowires obtained by a similar method by using DNA as template.²⁹ We explain the reduced conductivity by insufficient contact between the Pd particles; the distance between individual Pd nanoparticles is ca. 1 nm as it can be seen from the TEM image (Figure 1f).

CONCLUSIONS

In this paper, we report the fabrication of conductive nanowires using polymer bottle brushes as templates. In our approach, we synthesized poly(2-dimethylamino)ethyl methacrylate methyl iodide quaternary salt brushes by two-step atom transfer radical polymerization, loaded them with palladium salt, and reduced them in order to form metallic nanowires with average lengths and widths of 300 and 20 nm, respectively. The obtained nanowires were deposited between conductive gold pads and were connected to them by sputtering of additional pads to form an electric circuit. We connected the nanowires in an electric circuit and demonstrated that the conductivity of these nanowires is around $100 \text{ S}\cdot\text{m}^{-1}$, close to the conductivity of platinum bridges, fabricated by ion-beam deposition. We foresee a great potential of our approach for the design of nanoscale field-effect transistors and nanosensors.

Table 1. Electrical Resistivity and Conductivity of Bridge, Gap, and Nanowire Illustrated in Figure 3

object	resistance, M Ω	$S_{\text{cross-section}}$ nm ²	l , nm	resistivity, $\Omega\cdot\text{m}$	conductivity, S $\cdot\text{m}^{-1}$
bridge	0.86	10 400	1450	6×10^{-3}	167
gap	606				
nanowire	48	64	300	1×10^{-2}	98

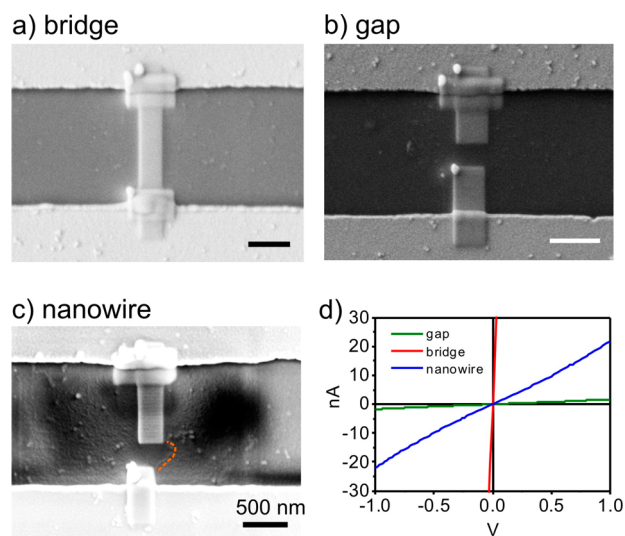


Figure 3. SEM images of bridge (a), gap (b), and bottle-brush-based nanowire (shown also with an orange dashed line) (c), as well as their Volt-Ampere characteristics (d). All scale bars are 500 nm.

■ ASSOCIATED CONTENT

Supporting Information

The Supporting Information is available free of charge on the ACS Publications website at DOI: 10.1021/acsami.5b07793.

Scheme of synthesis of polymer brushes; AFM images of native brushes, brushes after metallization, and exposure to plasma; optical and SEM images of substrates used for conductivity measurements; cross-section of AFM images of brushes before and after metallization. (PDF)

■ AUTHOR INFORMATION

Corresponding Author

*E-mail: ionov@uga.edu.

Notes

The authors declare no competing financial interest.

■ ACKNOWLEDGMENTS

The authors are grateful to DFG for financial support. Dr. Georgi Stoychev is acknowledged for CryoTEM experiments.

■ REFERENCES

- Li, Y.; Qian, F.; Xiang, J.; Lieber, C. M. Nanowire Electronic and Optoelectronic Devices. *Mater. Today* **2006**, *9* (10), 18–27.
- Thelander, C.; Agarwal, P.; Brongersma, S.; Eymery, J.; Feiner, L. F.; Forchel, A.; Scheffler, M.; Riess, W.; Ohlsson, B. J.; Gösele, U.; Samuelson, L. Nanowire-Based One-Dimensional Electronics. *Mater. Today* **2006**, *9* (10), 28–35.
- Cui, Y.; Wei, Q.; Park, H.; Lieber, C. M. Nanowire Nanosensors for Highly Sensitive and Selective Detection of Biological and Chemical Species. *Science* **2001**, *293* (5533), 1289–1292.
- Duan, X.; Huang, Y.; Cui, Y.; Wang, J.; Lieber, C. M. Indium Phosphide Nanowires as Building Blocks for Nanoscale Electronic and Optoelectronic Devices. *Nature* **2001**, *409* (6816), 66–69.

(5) Gudiksen, M. S.; Lauhon, L. J.; Wang, J.; Smith, D. C.; Lieber, C. M. Growth of Nanowire Superlattice Structures for Nanoscale Photonics and Electronics. *Nature* **2002**, *415* (6872), 617–620.

(6) Liang, Y.; Yokojima, S.; Ng, M.-F.; Chen, H.; He, G. Optical Properties of Single-Walled 4 Å Carbon Nanotubes. *J. Am. Chem. Soc.* **2001**, *123* (40), 9830–9836.

(7) Cao, H. Q.; Xu, Z.; Sang, H.; Sheng, D.; Tie, C. Y. Template Synthesis and Magnetic Behavior of an Array of Cobalt Nanowires Encapsulated in Polyaniline Nanotubes. *Adv. Mater.* **2001**, *13* (2), 121–123.

(8) Andres, R. P.; Bielefeld, J. D.; Henderson, J. I.; Janes, D. B.; Kolagunta, V. R.; Kubiak, C. P.; Mahoney, W. J.; Osifchin, R. G. Self-Assembly of a Two-Dimensional Superlattice of Molecularly Linked Metal Clusters. *Science* **1996**, *273* (5282), 1690–1693.

(9) Zhang, D.; Qi, L.; Ma, J.; Cheng, H. Formation of Silver Nanowires in Aqueous Solutions of a Double-Hydrophilic Block Copolymer. *Chem. Mater.* **2001**, *13* (9), 2753–2755.

(10) Song, J. H.; Wu, Y.; Messer, B.; Kind, H.; Yang, P. Metal Nanowire Formation Using Mo₃Se₃ as Reducing and Sacrificing Templates. *J. Am. Chem. Soc.* **2001**, *123* (42), 10397–10398.

(11) Han, Y.-J.; Kim, J. M.; Stucky, G. D. Preparation of Noble Metal Nanowires Using Hexagonal Mesoporous Silica SBA-15. *Chem. Mater.* **2000**, *12* (8), 2068–2069.

(12) Zach, M. P.; Ng, K. H.; Penner, R. M. Molybdenum Nanowires by Electrodeposition. *Science* **2000**, *290* (5499), 2120–2123.

(13) Morales, A. M.; Lieber, C. M. A Laser Ablation Method for the Synthesis of Crystalline Semiconductor Nanowires. *Science* **1998**, *279* (5348), 208–211.

(14) Govindaraj, A.; Satishkumar, B. C.; Nath, M.; Rao, C. N. R. Metal Nanowires and Intercalated Metal Layers in Single-Walled Carbon Nanotube Bundles. *Chem. Mater.* **2000**, *12* (1), 202–205.

(15) Jana, N. R.; Gearheart, L.; Murphy, C. J. Wet Chemical Synthesis of Silver Nanorods and Nanowires of Controllable Aspect Ratio. *Chem. Commun.* **2001**, *7*, 617–618.

(16) Verduzco, R.; Li, X.; Pesek, S. L.; Stein, G. E. Structure, Function, Self-Assembly, and Applications of Bottlebrush Copolymers. *Chem. Soc. Rev.* **2015**, *44* (8), 2405–2420.

(17) Sheiko, S. S.; Sumerlin, B. S.; Matyjaszewski, K. Cylindrical Molecular Brushes: Synthesis, Characterization, and Properties. *Prog. Polym. Sci.* **2008**, *33* (7), 759–785.

(18) Kiriya, A.; Gorodyska, G.; Minko, S.; Jaeger, W.; Štěpánek, P.; Stamm, M. Cascade of Coil-Globule Conformational Transitions of Single Flexible Polyelectrolyte Molecules in Poor Solvent. *J. Am. Chem. Soc.* **2002**, *124* (45), 13454–13462.

(19) Minko, S.; Kiriya, A.; Gorodyska, G.; Stamm, M. Mineralization of Single Flexible Polyelectrolyte Molecules. *J. Am. Chem. Soc.* **2002**, *124* (34), 10192–10197.

(20) Minko, S.; Kiriya, A.; Gorodyska, G.; Stamm, M. Single Flexible Hydrophobic Polyelectrolyte Molecules Adsorbed on Solid Substrate: Transition between a Stretched Chain, Necklace-like Conformation and a Globule. *J. Am. Chem. Soc.* **2002**, *124* (13), 3218–3219.

(21) Yuan, J.; Drechsler, M.; Xu, Y.; Zhang, M.; Müller, A. H. E. Cadmium Selenide Nanowires Within Core–Shell Cylindrical Polymer Brushes: Synthesis, Characterization and The Double-Loading Process. *Polymer* **2008**, *49* (6), 1547–1554.

(22) Zhang, M.; Drechsler, M.; Müller, A. H. E. Template-Controlled Synthesis of Wire-Like Cadmium Sulfide Nanoparticle Assemblies within Core–Shell Cylindrical Polymer Brushes. *Chem. Mater.* **2004**, *16* (3), 537–543.

(23) Djalali, R.; Li, S.-Y.; Schmidt, M. Amphipolar Core–Shell Cylindrical Brushes as Templates for the Formation of Gold Clusters and Nanowires. *Macromolecules* **2002**, *35* (11), 4282–4288.

(24) Müllner, M.; Lunkenbein, T.; Breu, J.; Caruso, F.; Müller, A. H. E. Template-Directed Synthesis of Silica Nanowires and Nanotubes from Cylindrical Core–Shell Polymer Brushes. *Chem. Mater.* **2012**, *24* (10), 1802–1810.

(25) Yuan, J.; Schacher, F.; Drechsler, M.; Hanisch, A.; Lu, Y.; Ballauff, M.; Müller, A. H. E. Stimuli-Responsive Organosilica Hybrid Nanowires Decorated with Metal Nanoparticles. *Chem. Mater.* **2010**, *22* (8), 2626–2634.

(26) Raguzin, I.; Stoychev, G.; Stamm, M.; Ionov, L. Single Molecule Investigation of Complexes of Oppositely Charged Bottle Brushes. *Soft Matter* **2013**, *9* (2), 359–364.

(27) Navaladian, S.; Viswanathan, B.; Varadarajan, T. K.; Viswanath, R. P. A Rapid Synthesis of Oriented Palladium Nanoparticles by UV Irradiation. *Nanoscale Res. Lett.* **2009**, *4* (2), 181–186.

(28) Liu, Z.; Zhan, Y.; Shi, G.; Moldovan, S.; Gharbi, M.; Song, L.; Ma, L.; Gao, W.; Huang, J.; Vajtai, R.; Banhart, F.; Sharma, P.; Lou, J.; Ajayan, P. M. Anomalous High Capacitance in a Coaxial Single Nanowire Capacitor. *Nat. Commun.* **2012**, *3*, 879.

(29) Braun, E.; Eichen, Y.; Sivan, U.; Ben-Yoseph, G. DNA-Templated Assembly and Electrode Attachment of a Conducting Silver Wire. *Nature* **1998**, *391* (6669), 775–778.